

The permanent ellipticity of the neutron star in PSR J1023+0038

Sudip Bhattacharyya^{*}

Department of Astronomy and Astrophysics, Tata Institute of Fundamental Research, Mumbai 400005, India

Accepted 2020 July 30. Received 2020 July 22; in original form 2020 June 11

ABSTRACT

A millisecond pulsar having an ellipticity, that is an asymmetric mass distribution around its spin-axis, could emit continuous gravitational waves, which have not been detected so far. An indirect way to infer such waves is to estimate the contribution of the waves to the spin-down rate of the pulsar. The transitional pulsar PSR J1023+0038 is ideal and unique for this purpose, because this is the only millisecond pulsar for which the spin-down rate has been measured in both accreting and non-accreting states. Here we infer, from our formalism based on the complete torque budget equations and the pulsar magnetospheric origin of observed γ -rays in the two states, that PSR J1023+0038 should emit gravitational waves due to a permanent ellipticity of the pulsar. The formalism also explains some other main observational aspects of this source in a self-consistent way. As an example, our formalism naturally infers the accretion disc penetration into the pulsar magnetosphere, and explains the observed X-ray pulsations in the accreting state using the standard and well-accepted scenario. This, in turn, infers the larger pulsar spin-down power in the accreting state, which, in our formalism, explains the observed larger γ -ray emission in this state. Exploring wide ranges of parameter values of PSR J1023+0038, and not assuming an additional source of stellar ellipticity in the accreting state, we find the misaligned mass quadrupole moment of the pulsar in the range of $(0.92 - 1.88) \times 10^{36}$ g cm², implying an ellipticity range of $(0.48 - 0.93) \times 10^{-9}$.

Key words: accretion, accretion discs — gravitational waves — pulsars: general — pulsars: individual (PSR J1023+0038) — stars: neutron — X-rays: binaries

1 INTRODUCTION

Observations and theoretical studies have indicated that millisecond pulsars (MSPs), i.e., rapidly spinning neutron stars which show periodic brightness oscillations, can have a misaligned mass distribution or ellipticity ($\epsilon \sim 10^{-9}$) around the spin-axis, and hence could emit gravitational waves continuously (Bildsten 1998; Andersson et al. 1999; Chakrabarty et al. 2003; Bhattacharyya & Chakrabarty 2017; Bhattacharyya 2017; Woan et al. 2018). But, so far only upper limits ($> 10^{-8}$) of ellipticity could be estimated using the Laser Interferometer Gravitational-Wave Observatory (LIGO; Abbott et al. 2019). However, a pulsar’s spin frequency (ν) and its rate of change ($\dot{\nu}$) can be measured from electromagnetic (e.g., radio, X-ray) observations, and an alternative way to infer gravitational waves is to estimate the contribution of these waves to the $\dot{\nu}$. While such an estimation could not be reliably achieved so far, PSR J1023+0038 (hereafter, J1023)

is an ideal pulsar for this study using torque ($= 2\pi\dot{\nu}I$; I is the stellar moment of inertia) budget calculations. This is because J1023 is one of the three known transitional MSPs, which are observed to swing between the non-accreting spin-powered radio MSP (RMSP) state and the accreting low-mass X-ray binary (LMXB) state (Archibald et al. 2009). Moreover, J1023 is unique because its $\dot{\nu}$ has been measured in both RMSP and LMXB states. In fact, based on the difference in $\dot{\nu}$ values in these two states, a model involving a stellar ellipticity only in the LMXB state was proposed (Haskell & Patruno 2017).

But a torque budget has hitherto not been systematically studied for J1023, although several classes of models have been proposed to explain its observational aspects. Here we briefly mention some of the noteworthy observational features and estimated parameter values of J1023. The spin frequency, mass (M) and distance of this pulsar or the neutron star, which may have an unevolved and Roche-lobe filling low-mass companion star of mass $\sim 0.2M_{\odot}$ (Thorstensen & Armstrong 2005; Archibald et al. 2010; Tendulkar et al. 2014), are 592.42 Hz,

* E-mail: sudip@tifr.res.in

$1.71 \pm 0.16 M_{\odot}$ and 1368_{-39}^{+42} pc respectively (Archibald et al. 2009; Deller et al. 2012). In the RMSP state, the companion star was found to be irradiated by the neutron star, which gave rise to an optical light curve with the orbital period of ~ 0.198094 days and with a peak-to-peak amplitude of ~ 0.3 magnitude, or a half-amplitude of ~ 180 K around a \sim G6 type star (Thorstensen & Armstrong 2005). Using a total binary system mass of $1.91 M_{\odot}$ and the measured orbital period, the binary separation a can be estimated. A 180 K half-amplitude around the 5590 K temperature of a G6 type companion star gives maximum and minimum temperatures: $T_{\max} = 5770$ K and $T_{\min} = 5410$ K. Then using the formula $4\pi a^2 \sigma (T_{\max}^4 - T_{\min}^4)$ (σ is the Stefan-Boltzmann constant), one can estimate a pulsar isotropic luminosity of at least 2.7×10^{33} erg s $^{-1}$. The irradiation was found to be similar in the LMXB state (Kennedy et al. 2018).

The measured spin-down rate $\dot{\nu}$ of J1023 in the RMSP state is $\approx -2.40 \times 10^{-15}$ Hz s $^{-1}$ (Deller et al. 2012; Archibald et al. 2013; Jaodand et al. 2016). However, considering the Shklovskii effect and the net effect of acceleration in the Galactic gravitational potential, the intrinsic spin-down rate in the RMSP state was estimated to be $\dot{\nu}_{\text{RMSP}} \approx -1.89 \times 10^{-15}$ Hz s $^{-1}$, which for a moment of inertia of 10^{45} g cm 2 gives a spin-down luminosity of $\sim 4.4 \times 10^{34}$ erg s $^{-1}$ (Deller et al. 2012; Archibald et al. 2013; Papitto & Torres 2015). In the RMSP state, a γ -ray luminosity ($L_{\gamma, \text{RMSP}}$) of $\sim 1.2 \times 10^{33}$ erg s $^{-1}$ was detected (Nolan et al. 2012; Papitto & Torres 2015). In the LMXB state, the γ -ray flux was observed to increase by a factor of $\sim 5 - 6.5$ relative to that in the RMSP state (Stappers et al. 2014; Deller et al. 2015). While this might imply a luminosity $L_{\gamma, \text{LMXB}} \approx (6.0 - 7.8) \times 10^{33}$ erg s $^{-1}$, Torres et al. (2017) reported $L_{\gamma, \text{LMXB}} \approx 12.4 \times 10^{33}$ erg s $^{-1}$. No radio pulsation was detected in the LMXB state (Deller et al. 2015). The presence of an accretion disc in the LMXB state was confirmed by the broad double-peaked H α emission line observed in the optical spectrum (Wang et al. 2009). The LMXB state X-ray luminosity (L_X), which is typically much higher than that in the RMSP state, has three distinctly different modes: low-mode ($L_X \sim 10^{33}$ erg s $^{-1}$), high-mode ($L_X \sim 7 \times 10^{33}$ erg s $^{-1}$) and flaring-mode ($L_X \sim 2 \times 10^{34}$ erg s $^{-1}$; Papitto & Torres 2015; Campana et al. 2016). The source typically spends $\sim 22\%$, $\sim 77\%$ and $\sim 1\%$ time in these modes respectively (Jaodand et al. 2016), and can switch between modes in ~ 10 s (Bogdanov et al. 2015). X-ray pulsations (rms amplitude $\sim 5 - 10\%$), i.e., a brightness variation of observed X-rays with the pulsar's spin period, have been detected only in the high-mode (Archibald et al. 2015; Jaodand et al. 2016). The spin-down rate $\dot{\nu}$ of the pulsar in the LMXB state, measured from X-ray pulsations, is $\approx -3.04 \times 10^{-15}$ Hz s $^{-1}$ (Jaodand et al. 2016). However, as for the RMSP state, the intrinsic spin-down rate in the LMXB state could be estimated to be $\dot{\nu}_{\text{LMXB}} \approx -2.50 \times 10^{-15}$ Hz s $^{-1}$. The X-ray behaviour of the source in low- and high-modes is exceptionally stable (Jaodand et al. 2016). Apart from X-ray pulsations, recently, optical pulsations at the pulsar spin frequency have also been discovered from J1023 in high and flaring modes in the LMXB state (Ambrosino et al. 2017). This is the first and so far the only MSP to show such optical pulsations. It was inferred that optical pulses were originated within a few kilometers from the location of the X-ray pulse origin (Papitto et al. 2019).

In this paper, we systematically study the torque budget, the energy budget and some other observational aspects of J1023, in order to find if the neutron star has a non-zero ellipticity. In section 2, we discuss the main classes of models proposed to explain the observational aspects of J1023. Section 3 describes our formalism in a simple manner, as well as our primary results, and section 4 discusses the feasibility of the formalism, and its implications. Together these two sections strongly suggest that the neutron star in J1023 can have an ellipticity. In section 5, we describe the method to constrain source parameter values using our formalism, and in section 6, we report the constrained ranges of parameter values. In section 7, we summarize our results and conclusions.

2 PREVIOUS MODELS OF PSR J1023+0038

In this section, we discuss some existing models of observational aspects of J1023. These not only could provide some motivations for our work, but also can be useful to explain our formalism.

The X-ray pulsations of J1023 in the high-mode of the LMXB state are similar to such a timing feature observed from accretion-powered millisecond X-ray pulsars (AMXPs). For AMXPs, X-ray pulsations are well-understood, and here we briefly describe this standard and well-accepted scenario, which requires an accretion disc. The disc is stopped by the pulsar dipolar magnetosphere at the magnetospheric radius (Patruno & Watts 2012, and references therein)

$$r_m = \xi \left(\frac{\mu^4}{2GM\dot{M}} \right)^{1/7}, \quad (1)$$

where, G is the gravitational constant, \dot{M} is the accretion rate, $\mu (= BR^3)$ is the pulsar magnetic dipole moment, B is the pulsar surface dipole magnetic field, R is the pulsar radius and ξ is an order of unity constant, which depends on the threading of the disc by the pulsar magnetic field lines (Wang 1996). In the 'accretion regime', when r_m is less than the corotation radius (Patruno & Watts 2012)

$$r_{\text{co}} = \left(\frac{GM}{4\pi^2\nu^2} \right)^{1/3}, \quad (2)$$

but greater than R and r_{ISCO} (innermost stable circular orbit (ISCO) radius), the accreted matter can be channelled to the pulsar's magnetic polar caps, giving rise to X-ray pulsations. On the other hand, for $r_{\text{lc}} > r_m > r_{\text{co}}$, i.e., in the 'propeller regime', accreted matter can be partially or fully driven away from the system (Patruno & Watts 2012). Here, $r_{\text{lc}} = c/2\pi\nu$ (≈ 80.5 km for J1023; c is the speed of light in vacuum) is the light cylinder radius.

But, does this mechanism for AMXPs work for the X-ray pulsations observed from J1023? Here, we mention independent observational indications. (1) J1023's X-ray pulsation characteristics are strikingly similar to those of the known AMXPs (Archibald et al. 2015), which suggests that they have the same pulsation mechanism. (2) A disc component was 6.1σ significant in the high-mode X-ray spectrum of J1023, as found from the *XMM-Newton* satellite data (Campana et al. 2016). This spectral analysis gave a disc inner edge radius (r_{in}) of 21_{-7}^{+9} km. From a later analysis with additional X-ray data, r_{in} was estimated to be

26_{-9}^{+11} km (Zelati et al. 2018). Both the spectral results suggest that the accretion disc could have extended inside the r_{co} ($\approx 24.6 - 26.2$ km, for $M \approx 1.55 - 1.87M_{\odot}$ for J1023) in the high mode, and hence the X-ray pulsations of J1023 might have the same origin as in other AMXPs.

However, if one assumes that the measured $\dot{\nu}_{\text{RMSP}}$ is entirely caused by the pulsar magnetospheric activities, the inferred high μ value ($\sim 10^{26}$ G cm³) implies that r_{m} is greater than r_{co} , and hence the requirement for the standard X-ray pulsation mechanism is not satisfied. An approach, which could allow a significantly lower value of r_{m} , i.e., $r_{\text{m}} < r_{\text{co}}$ even for $\mu \sim 10^{26}$ G cm³ for J1023, was discussed in Bozzo et al. (2018). But this paper mentioned that such an approach could not explain other phenomena observed in the LMXB state of J1023. Therefore, almost none of the major existing models for J1023 can accommodate the standard and well-accepted mechanism for X-ray pulsations in the LMXB state, as all of them use a relatively high μ value inferred from the measured $\dot{\nu}_{\text{RMSP}}$. Now we briefly mention some classes of these existing models.

One class of such models assumes that the pulsar magnetospheric activities operate at the same level in both RMSP and LMXB states. Therefore, this class of models cannot explain a significantly higher $|\dot{\nu}_{\text{LMXB}}|$ value compared to the $|\dot{\nu}_{\text{RMSP}}|$ value, based on such equal magnetospheric activities. Some of these models attempt to explain observed X-ray properties in the LMXB state in terms of the spin power of the pulsar (Stappers et al. 2014; Takata et al. 2014). However, while these models might explain the higher γ -ray luminosity value in the LMXB state, most of them may not explain the remarkably stable LMXB X-ray modes and fast switching between them, X-ray pulsations only in the high-mode, X-ray pulse profiles (see Papitto & Torres 2015), and the measured low disc inner edge radius r_{in} (Campana et al. 2016).

Another type of models involves a high accretion rate (\dot{M}), about a hundred times the value inferred from X-ray observations, in the high-mode of J1023 (Papitto & Torres 2015). According to such a model, r_{in} is close to but greater than r_{co} , and hence the source is in the propeller regime in the high-mode (Campana et al. 2016). Since matter is propelled away from the system in the propeller regime, it is claimed that $\sim 99\%$ of the disc matter is accelerated and ejected from J1023 (Papitto & Torres 2015). This might explain the $\sim 5 - 6.5$ times higher γ -ray luminosity in the LMXB state. However, this would also imply a $|\dot{\nu}_{\text{LMXB}}|$ value at least twice the $|\dot{\nu}_{\text{RMSP}}|$ value (Papitto & Torres 2015), which is much higher than that observed (see also Papitto et al. 2019). Note that this model might imply an even higher $|\dot{\nu}_{\text{LMXB}}|$ value, if $L_{\gamma, \text{LMXB}} \approx 12.4 \times 10^{33}$ erg s⁻¹, reported by Torres et al. (2017) (see section 1), is considered. Besides, it may not be possible to expel $\sim 99\%$ of the disc matter by propeller activities when r_{in} is *not* much higher than r_{co} (see Campana et al. 2016), as most of this matter would come back and accumulate, thus making the disc extend inside r_{co} (D’Angelo & Spruit 2010). This would result in a much higher L_{X} than that observed, and a large spin-up torque which is not observed. In this $\sim 99\%$ accreted matter ejection model, even for $r_{\text{m}} > r_{\text{co}}$, the X-ray luminosity might be much higher than the observed high-mode X-ray luminosity (see Veledina et al. 2019). Besides, such a model may not explain the remarkable stability of

the high-mode, as even a very small fractional change in the $\sim 99\%$ expelled matter would change the $\sim 1\%$ accreting matter by a large fraction. Moreover, this model relies on the disc-magnetosphere interaction which should not drastically change from one system to another, as long as the neutron star μ and ν values and the \dot{M} value are not very different. Therefore, if the accretion rate is indeed so high at such a low X-ray luminosity of J1023, $\sim 99\%$ of this accreted matter is propelled away to give rise to an enhanced γ -ray luminosity, and $\sim 1\%$ of this accreted matter gives rise to X-ray pulsations, we would expect to observe such features from the known AMXPs with similar μ values ($\sim 10^{26}$ G cm³) at similarly low X-ray luminosities. But, these have not been observed. Due to all these reasons, we conclude that an accretion rate much higher than the one indicated by the observed X-ray luminosity, and the corresponding propeller effect, may not explain the LMXB state of J1023.

Another type of model (Haskell & Patruno 2017) attempts to explain the difference between $\dot{\nu}_{\text{RMSP}}$ and $\dot{\nu}_{\text{LMXB}}$, assuming an extra spin-down torque due to gravitational waves emitted from the neutron star *only* in the LMXB state. However, this paper (Haskell & Patruno 2017) does not address other major observational aspects of J1023 in the LMXB state, such as the higher γ -ray luminosity, stability and fast switching of modes, and X-ray pulsations only in the high-mode. Moreover, while this model requires accretion onto the neutron star in the LMXB state, it also implicitly assumes a relatively high μ value inferred from the measured $\dot{\nu}_{\text{RMSP}}$. However, it is not discussed how the accreted matter would reach the neutron star surface for such a high μ value. Besides, if the accretion disc comes close to the neutron star, at least a fraction of the magnetic field lines intersecting the disc should be opened (reported from simulations; see Parfrey et al. 2016; Parfrey & Tchekhovskoy 2017), and would likely increase the spin-down torque by several times, relative to the torque in the RMSP state, due to enhanced pulsar magnetospheric activities (section 4.3 discusses this point in more detail). Note that here we consider these activities are not quenched in the LMXB state, as Haskell & Patruno (2017) implicitly assume. Such an additional spin-down torque would imply a higher value of $|\dot{\nu}_{\text{LMXB}}|$ than the one inferred (see section 1). Moreover, in this case a spin-down torque due to gravitational waves, which is the main proposition of Haskell & Patruno (2017), would not be required anyway. On the other hand, if pulsar magnetospheric activities are quenched in the LMXB state, the γ -ray luminosity in this state cannot be explained. Therefore, we conclude that the gravitational wave emission *only* in the LMXB state may not explain the torque budget and other properties of J1023. In fact, Singh et al. (2020) have recently shown that a large enough ellipticity, required to explain the increase of the spin-down rate in the LMXB state of J1023, cannot be built only during the accretion phase, unless strong shallow heating layers are present.

Recently, two models have been proposed to explain some properties of J1023, including the optical pulsations at the pulsar spin frequency (Veledina et al. 2019; Papitto et al. 2019). Both these models assume that the pulsar magnetosphere remains active in the LMXB state, the disc is truncated outside the light cylinder in the high-mode, and optical and X-ray pulses are produced by synchrotron

emission from the dissipative collision between a rotating pulsar wind and the inner edge cross section of the accretion disc. This mechanism is highly non-standard to explain the X-ray pulsations from an accreting MSP. Besides, an accretion disc outside the light cylinder radius (≈ 80.5 km) cannot explain a disc component found with 6.1σ significance, the inner edge radius of which has been inferred to be 21_{-7}^{+9} km (Campana et al. (2016); and 26_{-9}^{+11} km using later data; Zelati et al. (2018)) from the high-mode X-ray spectrum (see section 1).

According to the model of Veledina et al. (2019), the accretion disc penetrates the light cylinder during the low-mode in the LMXB state, but r_m remains greater than r_{co} . This can open up additional pulsar magnetic field lines and increase the spin-down torque at most by a factor of $(r_{lc}/r_m)^2$ (Parfrey et al. 2016). This is the way Veledina et al. (2019) attempt to explain the increase of the average spin-down rate in the LMXB state. However for this, an evacuation of almost all the accreted matter from the light cylinder has to happen in ~ 10 s during the low-to-high mode transition, so that the equatorial part of the pulsar wind is switched on to begin the high-mode, according to this model. Moreover, during every such transition, first the X-ray luminosity is expected to decrease as the disc moves outwards, and then to sharply increase as the wind-disc collision happens. On the other hand, during every high-to-low mode transition, the X-ray luminosity should first decrease sharply as the equatorial pulsar wind is shut down, and then somewhat increase as the disc extends inwards inside the magnetosphere. This could be tested using X-ray data with sufficient time resolution and statistics.

A main difference of the model of Papitto et al. (2019) with that of Veledina et al. (2019) is regarding the low-mode in the LMXB state. According to Papitto et al. (2019), the accretion disc is pushed away even farther from the pulsar in the low-mode, without any change in the pulsar's magnetosphere and the accretion process. Since, the pulsar magnetospheric activities should remain same in RMSP and LMXB states for this model, Papitto et al. (2019) would not perhaps explain the significantly higher $|\dot{\nu}_{\text{LMXB}}|$ value compared to the $|\dot{\nu}_{\text{RMSP}}|$ value.

We, therefore, conclude that no existing model can explain the energy budget and torque budget of J1023, using the standard scenario of X-ray pulsations in the LMXB state.

3 FORMALISM AND PRIMARY RESULTS

In this section, we introduce our formalism using specific values of measured source parameters, as well as typical values of other neutron star parameters. This will be useful to demonstrate, in a simple manner, how this formalism works for J1023, and will probe if the neutron star emits gravitational waves. In section 5, we will describe the method to estimate the allowed ranges of several source parameter values in a robust way, considering the full ranges of measured and unknown input source parameter values.

3.1 Implications of torque budget equations

The energy budget and the torque budget of an MSP, which are related to energy and angular momentum conservations respectively, are the most important observational physical aspects, which any successful model must explain. Unlike some other models, our formalism for J1023 is based on this requirement. Particularly, to the best of our knowledge, J1023 is so far the only MSP for which the time derivatives of the spin frequency both in RMSP and LMXB states have been measured. So, we start by utilizing this unique information, and write the torque budget equations in the two states. Note that, in the RMSP state, there could be only two types of torque: due to pulsar wind and electromagnetic radiation from the pulsar magnetosphere (Lyne & Graham-Smith 2012) and gravitational waves from the pulsar (Abbott et al. 2019). During the LMXB state, only one additional type of torque can be present, i.e., due to the accreted/ejected matter. Since in the following torque budget equations for J1023, we include terms due to all these types of torque, these are the most general torque budget equations without assumptions and irrespective of other observational aspects. Using the intrinsic values mentioned in section 1, we get for the RMSP state,

$$\dot{\nu}_{\text{RMSP}}^{\text{PW}} + \dot{\nu}_{\text{RMSP}}^{\text{GW}} = \dot{\nu}_{\text{RMSP}} = -1.89 \times 10^{-15} \text{ Hz s}^{-1}, \quad (3)$$

and for the LMXB state,

$$\dot{\nu}_{\text{LMXB}}^{\text{PW}} + \dot{\nu}_{\text{LMXB}}^{\text{GW}} + \dot{\nu}_{\text{LMXB}}^{\text{Acc}} = \dot{\nu}_{\text{LMXB}} = -2.50 \times 10^{-15} \text{ Hz s}^{-1}. \quad (4)$$

Here, $\dot{\nu}$ is the rate of change of the neutron star spin frequency, which is related to the torque (N) by $N = 2\pi\dot{\nu}I$, where I is the stellar moment of inertia (section 1). The subscripts ‘RMSP’ and ‘LMXB’ indicate the RMSP and LMXB states respectively, while the superscripts ‘PW’, ‘GW’ and ‘Acc’ denote torques due to pulsar magnetospheric activities, gravitational waves and accretion/ejection respectively.

In Eqs. 3 and 4, we include terms due to gravitational waves, i.e., $\dot{\nu}_{\text{RMSP}}^{\text{GW}}$ and $\dot{\nu}_{\text{LMXB}}^{\text{GW}}$. This is because a neutron star could support a certain amount of ellipticity around its spin axis (Johnson-McDaniel & Owen 2013), and hence could spin down due to gravitational wave emission. In fact, a population-based study of non-accreting MSPs indicated that such sources could have an ellipticity of $\sim 10^{-9}$ with respect to their spin-axis (Woan et al. 2018). However, to the best of our knowledge, all the previous models for J1023 implicitly assumed $\dot{\nu}_{\text{RMSP}}^{\text{GW}} = 0$, and almost all the previous models (except that of Haskell & Patruno 2017) implicitly assumed $\dot{\nu}_{\text{LMXB}}^{\text{GW}} = 0$, without providing a reason. We make our formalism more complete by including these terms. But, we emphasize that we do not a priori assume non-zero values of $\dot{\nu}_{\text{RMSP}}^{\text{GW}}$ and $\dot{\nu}_{\text{LMXB}}^{\text{GW}}$. Rather, we estimate their values by solving Eqs. 3 and 4. For this, let us first examine the other terms ($\dot{\nu}_{\text{LMXB}}^{\text{Acc}}$, $\dot{\nu}_{\text{RMSP}}^{\text{PW}}$, $\dot{\nu}_{\text{LMXB}}^{\text{PW}}$) in these equations.

The relatively low X-ray luminosity of J1023 implies a low accretion rate and hence a low value of $|\dot{\nu}_{\text{LMXB}}^{\text{Acc}}|$ in Eq. 4. While an unusual model of higher accretion rate, with $\sim 99\%$ accreted matter ejected from the system, was proposed mainly to explain the increased γ -ray emission in the LMXB state (Papitto & Torres 2015), it has been argued in section 2 that an accretion rate much higher than the one indicated by the observed X-ray luminosity cannot gener-

ally explain the LMXB state of J1023. So, using a typical X-ray luminosity value of the LMXB state, $|\dot{\nu}_{\text{LMXB}}^{\text{Acc}}|$ can be shown to be only a few percent of $|\dot{\nu}_{\text{LMXB}}|$ in a simple way. In sections 4.2 and 6, we will estimate $\dot{\nu}_{\text{LMXB}}^{\text{Acc}}$ in more detail, averaging over all three modes, and find that it is positive and at most $\sim 5\%$ of $|\dot{\nu}_{\text{LMXB}}|$.

Next, we consider the terms $\dot{\nu}_{\text{RMSP}}^{\text{PW}}$ and $\dot{\nu}_{\text{LMXB}}^{\text{PW}}$ in Eqs. 3 and 4. As we will discuss in more detail in section 4, γ -rays emitted in both RMSP and LMXB states of J1023 should be powered by the pulsar spin energy through the pulsar wind and the electromagnetic radiation from the pulsar magnetosphere. This is the standard energy source of a pulsar's γ -ray emission, and no other energy source for γ -rays is known to be available in J1023. Note that, while the pulsar spin energy could power the γ -rays in the LMXB state through $\sim 99\%$ accreted matter ejected from the system with high velocities (Papitto & Torres 2015), this model may not explain the LMXB state of J1023 (see section 2). Therefore, since the pulsar spin energy powers the γ -ray emission and hence this emission partially causes the spin-down of the pulsar, $\dot{\nu}_{\text{RMSP}}^{\text{PW}}$ and $\dot{\nu}_{\text{LMXB}}^{\text{PW}}$ should be related to the γ -ray luminosities ($L_{\gamma,\text{RMSP}}$ and $L_{\gamma,\text{LMXB}}$) in RMSP and LMXB states of J1023, as shown by the next two equations. The pulsar spin-down power in the RMSP state due to magnetospheric outflow and emission is

$$L_{\text{SD, RMSP}}^{\text{PW}} = -4\pi^2 I \nu \dot{\nu}_{\text{RMSP}}^{\text{PW}} = L_{\gamma,\text{RMSP}} / \eta_{\text{RMSP}}, \quad (5)$$

where, η_{RMSP} is the γ -ray emission efficiency in the RMSP state. Similarly, the pulsar spin-down power in the LMXB state due to magnetospheric outflow and emission is

$$L_{\text{SD, LMXB}}^{\text{PW}} = -4\pi^2 I \nu \dot{\nu}_{\text{LMXB}}^{\text{PW}} = L_{\gamma,\text{LMXB}} / \eta_{\text{LMXB}}, \quad (6)$$

where, η_{LMXB} is the γ -ray emission efficiency in the LMXB state. From Eqs. 5 and 6, we can write

$$\frac{L_{\text{SD, LMXB}}^{\text{PW}}}{L_{\text{SD, RMSP}}^{\text{PW}}} = \frac{\dot{\nu}_{\text{LMXB}}^{\text{PW}}}{\dot{\nu}_{\text{RMSP}}^{\text{PW}}} = \frac{L_{\gamma,\text{LMXB}} / L_{\gamma,\text{RMSP}}}{\eta_{\text{LMXB}} / \eta_{\text{RMSP}}}. \quad (7)$$

With this information about the terms $\dot{\nu}_{\text{LMXB}}^{\text{Acc}}$, $\dot{\nu}_{\text{RMSP}}^{\text{PW}}$ and $\dot{\nu}_{\text{LMXB}}^{\text{PW}}$, let us first examine from Eqs. 3 and 4 in an almost model-independent way, if $\dot{\nu}_{\text{RMSP}}^{\text{GW}}$ and/or $\dot{\nu}_{\text{LMXB}}^{\text{GW}}$ can be zero. This is because, if we can show in a model-independent way that at least one of them cannot be zero, then we can reliably infer a non-zero ellipticity of and the gravitational wave emission from the neutron star. We call this an almost model-independent way, because we use primarily some observational knowledge and the general torque budget equations (Eqs. 3 and 4), and these equations should be valid for any model. Considering $L_{\gamma,\text{LMXB}} / L_{\gamma,\text{RMSP}} \geq 5$ (see section 1) in Eq. 7, it can be easily seen from Eqs. 3 and 4 that $|\dot{\nu}_{\text{RMSP}}^{\text{GW}}|$ has to be greater than zero for $\dot{\nu}_{\text{LMXB}}^{\text{GW}} = 0$ and $\eta_{\text{LMXB}} / \eta_{\text{RMSP}} \lesssim 3.5$, implying gravitational wave emission from the pulsar in the RMSP state. Note that this upper limit of $\eta_{\text{LMXB}} / \eta_{\text{RMSP}}$, for which $|\dot{\nu}_{\text{RMSP}}^{\text{GW}}|$ has to be greater than zero, is higher for $|\dot{\nu}_{\text{LMXB}}^{\text{GW}}| > 0$.

Since the conclusion of $|\dot{\nu}_{\text{RMSP}}^{\text{GW}}| > 0$ is valid only for a range of $\eta_{\text{LMXB}} / \eta_{\text{RMSP}}$, how reliable is it? In other words, what values of $\eta_{\text{LMXB}} / \eta_{\text{RMSP}}$ do we expect? Note that, while the γ -ray emission should be powered by the pulsar spin energy through the pulsar wind and the electromagnetic radiation from the pulsar magnetosphere, there could be multiple γ -ray production mechanisms. This means, γ -rays may

be produced either directly from the magnetospheric outflow and emission (i.e., the γ -ray emission is a part of the pulsar magnetospheric emission), or by an additional mechanism (e.g., by a pulsar wind – accretion disc collision; see section 2), or both. If the γ -ray emission in each of RMSP and LMXB states is a part of the pulsar magnetospheric emission, and since $L_{\gamma,\text{LMXB}} > L_{\gamma,\text{RMSP}}$, it is reasonable to consider that $L_{\text{SD, LMXB}}^{\text{PW}} > L_{\text{SD, RMSP}}^{\text{PW}}$ for J1023 (section 4.3 will discuss a mechanism for $L_{\text{SD, LMXB}}^{\text{PW}} > L_{\text{SD, RMSP}}^{\text{PW}}$). Hence, $\eta_{\text{LMXB}} / \eta_{\text{RMSP}} < 1$, as the γ -ray efficiency is expected to decrease with the increase of the pulsar spin-down power (Lyne & Graham-Smith 2012). Therefore, if the γ -ray emission in each of RMSP and LMXB states is a part of the pulsar magnetospheric emission, then from the above it appears inevitable that $|\dot{\nu}_{\text{RMSP}}^{\text{GW}}| > 0$, and the neutron star in J1023 has a non-zero ellipticity and emits gravitational waves in the RMSP state.

The other option, i.e., $\eta_{\text{LMXB}} / \eta_{\text{RMSP}} \geq 1$, typically implies that at least a fraction of γ -ray emission in the LMXB state is produced by an additional mechanism (e.g., by a pulsar wind – accretion disc collision; see section 2). Therefore, since $|\dot{\nu}_{\text{RMSP}}^{\text{GW}}| > 0$ for $\eta_{\text{LMXB}} / \eta_{\text{RMSP}} \lesssim 3.5$, the neutron star in J1023 may emit gravitational waves in the RMSP state, even if a considerable fraction of γ -rays in the LMXB state is produced by such an additional mechanism. Nevertheless, it is important to enquire if γ -rays in each of RMSP and LMXB states are actually a part of the pulsar magnetospheric emission, because in this case the gravitational wave emission in the RMSP state appears to be certain. While there is no independent observational evidence of such a direct pulsar magnetospheric production of γ -rays in both states, in section 4.4 we will argue that this production is the simplest explanation for γ -rays, has not been falsified yet, is feasible, explains some properties of J1023 better than alternative mechanisms, and also allows a self-consistent scenario to understand the main observational aspects of J1023.

Note that, if the neutron star in J1023 has a non-zero ellipticity in the RMSP state, it is unlikely to disappear in the LMXB state (section 6 includes a brief discussion). Therefore, if $|\dot{\nu}_{\text{RMSP}}^{\text{GW}}| > 0$, $|\dot{\nu}_{\text{LMXB}}^{\text{GW}}|$ is also expected to be greater than zero. In fact, considering ranges of parameter values and additional observational constraints, we will report in section 6 that both $|\dot{\nu}_{\text{RMSP}}^{\text{GW}}|$ and $|\dot{\nu}_{\text{LMXB}}^{\text{GW}}|$ are greater than zero.

3.2 Results for specific parameter values

Considering the above mentioned formalism and for typical input parameter values, now we solve Eqs. 3, 4 and 7, in order to find out reasonable values of some source parameters. We consider that $L_{\gamma,\text{LMXB}} / L_{\gamma,\text{RMSP}} = 6.5$ (see section 1) and $\eta_{\text{LMXB}} / \eta_{\text{RMSP}} = 1$. We will explore reasonable ranges of these parameters in section 5. Therefore, from Eq. 7, we get $\dot{\nu}_{\text{LMXB}}^{\text{PW}} / \dot{\nu}_{\text{RMSP}}^{\text{PW}} = 6.5$. Here, we ignore the relatively small term $\dot{\nu}_{\text{LMXB}}^{\text{Acc}}$ in Eq. 4, as this term does not affect the results much. However, we will include this term in a self-consistent way in sections 5 and 6. Here, we also consider $\dot{\nu}_{\text{LMXB}}^{\text{GW}} = \dot{\nu}_{\text{RMSP}}^{\text{GW}}$. In sections 5 and 6, we will explore the possibility of $\dot{\nu}_{\text{LMXB}}^{\text{GW}} \neq \dot{\nu}_{\text{RMSP}}^{\text{GW}}$.

Therefore, solving Eqs. 3 and 4, we get $\dot{\nu}_{\text{RMSP}}^{\text{PW}} = -0.111 \times 10^{-15} \text{ Hz s}^{-1}$ and $\dot{\nu}_{\text{RMSP}}^{\text{GW}} = \dot{\nu}_{\text{LMXB}}^{\text{GW}} = -1.779 \times 10^{-15} \text{ Hz s}^{-1}$. The torque corresponding to $\dot{\nu}_{\text{RMSP}}^{\text{PW}}$ is given

by (see [Lyne & Graham-Smith 2012](#))

$$2\pi\dot{\nu}_{\text{RMSP}}^{\text{PW}}I = -\frac{2\mu^2 \sin^2 \alpha (2\pi\nu)^n}{3c^3}, \quad (8)$$

where n and α are the pulsar braking index and the angle between the magnetic and spin axes, respectively. The torque corresponding to $\dot{\nu}_{\text{RMSP}}^{\text{GW}}$ is given by (see [Bhattacharyya 2017](#))

$$2\pi\dot{\nu}_{\text{RMSP}}^{\text{GW}}I = -\frac{32GQ^2}{5} \left(\frac{2\pi\nu}{c}\right)^5, \quad (9)$$

where Q is the misaligned mass quadrupole moment of the pulsar. Assuming typical parameter values, viz., $I = 2 \times 10^{45}$ g cm², $n = 3$ and $\alpha = 60^\circ$, we get $\mu \approx 3.8 \times 10^{25}$ G cm³ and $Q \approx 1.33 \times 10^{36}$ g cm² from Eqs. 8 and 9. For a neutron star radius (R) of 14 km and the same I -value, these imply the stellar surface dipole magnetic field $B = \mu/R^3 \approx 1.39 \times 10^7$ G and ellipticity $\epsilon = Q/I \approx 0.67 \times 10^{-9}$.

4 FEASIBILITY AND IMPLICATIONS

In this section, we briefly discuss the feasibility of our formalism (section 3), and its implications for various observational aspects.

4.1 General aspects

First, we note that J1023 can be a spin-powered pulsar, if $B_{12}\nu^2 > 0.2$ ($B_{12} = B/10^{12}$ G; [Bhattacharyya & van den Heuvel 1991](#)). This condition is well satisfied for the estimated B value mentioned in section 3.2. The estimated Q and ϵ values are also consistent with the limits indicated for MSPs in [Bhattacharyya \(2017\)](#); [Woan et al. \(2018\)](#).

From the numbers mentioned in section 3.2, $L_{\text{SD,RMSP}}^{\text{PW}} = 5.2 \times 10^{33}$ erg s⁻¹ (using Eq. 5). This may explain the observed irradiation of the companion star, which requires a pulsar isotropic luminosity of at least 2.7×10^{33} erg s⁻¹ (see section 1). The γ -ray emission efficiency ($\eta_{\text{RMSP}} = L_{\gamma,\text{RMSP}}/L_{\text{SD,RMSP}}^{\text{PW}}$) in the RMSP state is ~ 0.23 (from section 3.2), which is consistent with the values for the *Fermi*-LAT-detected MSPs ([Abdo et al. 2013](#)).

4.2 Aspects of accretion

Let us now examine what our formalism and the corresponding reasonable parameter values (see section 3.2) imply for the LMXB state of J1023. Using $L_X = 7 \times 10^{33}$ erg s⁻¹ (see section 1) and the usual factor of accreted mass to X-ray energy conversion (i.e., GM/R ; $M = 1.71M_\odot$ and $R = 14$ km; sections 1 and 3.2) in the high-mode, we get the accretion rate $\dot{M} \sim 4.3 \times 10^{13}$ g s⁻¹. Then, using Eq. 1, $\xi = 0.3$ and $\mu = 3.8 \times 10^{25}$ G cm³ (see section 3.2), we get the magnetospheric radius $r_{\text{m,high}}$ in the high-mode to be ≈ 24.6 km. This is less than r_{co} ($= 25.4$ km in this case; Eq. 2), greater than both R and r_{ISCO} (~ 15.4 km), and hence satisfies the condition for standard X-ray pulsation mechanism (see section 2). Therefore, our formalism can explain the X-ray pulsations of J1023 during the high-mode using the standard and well-accepted scenario, although this formalism is based

on the torque budget and γ -ray luminosities, and is independent of X-ray pulsations. In fact, our formalism in section 3.1 does not include the accretion at all, except, based on a low observed X-ray luminosity, the magnitude of the accretion/ejection torque in the LMXB state is considered to be small in comparison to the total torque magnitude. Besides, since the above values imply that the accreted matter falls on the neutron star surface in the high-mode, it is justified to use GM/R as the factor of accreted mass to X-ray energy conversion. It is also important to note that the above $r_{\text{m,high}}$ value is fully consistent with the disc inner edge radius ($r_{\text{in}} = 21_{-7}^{+9}$ km; [Campana et al. \(2016\)](#); $r_{\text{in}} = 26_{-9}^{+11}$ km; [Zelati et al. \(2018\)](#)) in the high-mode, which was independently measured from X-ray spectral analysis. Therefore, the fact that our formalism can predict X-ray pulsations and r_{in} values, which are independently observed and measured for the high-mode, strongly supports this formalism and the conclusions described in section 3.

Here, we note that, unlike many other models, our formalism leads to the accretion onto the neutron star in the high-mode, because the μ -values in our scenario come out to be lower than those estimated assuming $\dot{\nu}_{\text{RMSP}}^{\text{PW}} = \dot{\nu}_{\text{RMSP}}$. This is because we obtain a substantial non-zero value for $\dot{\nu}_{\text{RMSP}}^{\text{GW}}$, and hence $|\dot{\nu}_{\text{RMSP}}^{\text{PW}}| < |\dot{\nu}_{\text{RMSP}}|$ (see Eq. 3) for our formalism.

Let us now consider the low-mode. Using Eq. 1, the above mentioned parameter values (i.e., $M = 1.71M_\odot$, $\xi = 0.3$, $\mu = 3.8 \times 10^{25}$ G cm³; sections 1 and 3.2), $L_X = 10^{33}$ erg s⁻¹ (see section 1) and the factor of accreted mass to X-ray energy conversion as $GM/2r_{\text{m,low}}$ ($r_{\text{m,low}}$ is the magnetospheric radius in the low-mode), we find $\dot{M} \sim 2.5 \times 10^{13}$ g s⁻¹ and $r_{\text{m,low}} \approx 28.7$ km. This implies $r_{\text{lc}} > r_{\text{m,low}} > r_{\text{co}}$ and J1023 is in the propeller regime in the low-mode (see section 2), which explains why X-ray pulsations are not observed in this mode. Moreover, since in this propeller regime the accreted matter should not reach the neutron star surface, an energy conversion factor of $GM/2r_{\text{m,low}}$ is justified. Note that, had we used an energy conversion factor of GM/R , $r_{\text{m,low}}$ would be greater than 28.7 km, and the accreted matter would not reach the stellar surface anyway. Therefore, GM/R is not justified as the energy conversion factor in the low-mode, as GM/R can be used only when the matter falls on the stellar surface. From the above we find that, although the solutions of Eqs. 3, 4 and 7 do not use the accretion phenomenon apart from considering the accretion/ejection torque magnitude to be small relative to the total torque magnitude, they lead to the conclusion that J1023 is in the accretion regime in the high-mode and in the propeller regime in the low-mode. These two different regimes naturally explain the two distinctly different modes (high and low) of the LMXB state of J1023.

As can be seen from the values of $r_{\text{m,high}}$ and $r_{\text{m,low}}$, a mode change requires the disc to move only by a few km and to cross the r_{co} . This can happen in the viscous time scale $t_{\text{visc}} \sim \alpha^{-1}(H/r)^{-2}(r^3/GM)^{1/2}$ ([Veledina et al. 2019](#)). Here, α is the Shakura-Sunyaev viscosity parameter and H is the height of the disc at a radial distance r . We consider $r \sim r_{\text{co}} \sim 25$ km and $M \sim 1.71M_\odot$, and find that $t_{\text{visc}} \sim 3(\alpha/0.01)^{-1}(r/10H)^2$ s, which can comfortably explain the observed fast switch between modes (section 1).

The disc is truncated close to the r_{co} , which is expected for a mechanism discussed in [D'Angelo & Spruit](#)

(2010) (also see Bhattacharyya & Chakrabarty 2017), and could explain the stability of X-ray intensity in each of high- and low-modes. Since r_{co} , being a function of only M and ν (Eq. 2), does not appreciably change within a few years, the X-ray intensity in each mode could remain stable over the years, as observed (Jaodand et al. 2016).

The approximate magnitude of the torque ($|\dot{\nu}_{\text{LMXB}}^{\text{Acc}}|$; see Eq. 4) due to accretion/ejection can be estimated from the formula $|\dot{M}\sqrt{GM/r_m}|$ for each mode of the LMXB state (Bhattacharyya & Chakrabarty 2017). We consider a spin-up torque for the high and flaring modes, with percentage durations of $\sim 77\%$ and $\sim 1\%$ respectively. For the low-mode, we consider a spin-down torque using the above formula, and a percentage duration of $\sim 22\%$. These give a net time derivative of spin frequency ($\dot{\nu}_{\text{LMXB}}^{\text{Acc}}$), averaged over the entire LMXB state, of $\sim 5.3 \times 10^{-17} \text{ Hz s}^{-1}$ (for parameter values mentioned in sections 1 and 3.2). This value of $\dot{\nu}_{\text{LMXB}}^{\text{Acc}}$ is only $\sim 2.1\%$ of $|\dot{\nu}_{\text{LMXB}}|$, and hence its omission in a simple calculation is justified (see section 3). Note that, depending on the extent of the interaction of the neutron star magnetic field with the disc, and what fraction of the accreted matter can escape from the system by the propeller effect in the low-mode, $\dot{\nu}_{\text{LMXB}}^{\text{Acc}}$ could have an uncertainty by a large fraction, but it would still remain a small fraction of $|\dot{\nu}_{\text{LMXB}}|$.

4.3 Aspects of γ -ray emission

Let us now discuss the feasibility of γ -ray emission being powered by the pulsar spin energy through the pulsar magnetospheric activities in both RMSP and LMXB states of J1023, as considered in our formalism (section 3.1). In the RMSP state, the pulsar is clearly active, and hence γ -rays can easily be powered by the pulsar spin energy through the magnetospheric activities. In fact, this is the standard scenario of γ -ray origin for a radio MSP. However, it is usually believed that pulsar magnetospheric activities are switched off due to accretion in an LMXB. But, it has been seen from recent simulations that such activities could continue even when the accreted matter reaches the neutron star surface (Parfrey et al. 2016; Parfrey & Tchekhovskoy 2017). This can happen when a low accretion rate, corresponding to a low X-ray luminosity, cannot quench the pulsar activities. We note that this could happen for J1023, as its average X-ray luminosity in the LMXB state is less than $10^{34} \text{ erg s}^{-1}$, while the quenching luminosity was estimated to be $\gtrsim 5 \times 10^{35} \text{ erg s}^{-1}$ (Zelati et al. 2014). Note that, for other AMXPs, the X-ray luminosity is typically higher than $5 \times 10^{35} \text{ erg s}^{-1}$ in the accretion phase, and hence the pulsar activities can be quenched. Therefore, the pulsar magnetospheric activities can continue in the LMXB state of J1023, and the γ -ray emission powered by the pulsar spin energy in this state is feasible.

But is it feasible that γ -rays are produced directly from the magnetospheric outflow and emission, i.e., the γ -ray emission is a part of the pulsar magnetospheric emission, in both RMSP and LMXB states of J1023? For the RMSP state, this is feasible, and the γ -ray emission, similar to such emissions from many other MSPs detected with the *Fermi* Large Area Telescope (LAT), is in fact believed to be a part of the pulsar magnetospheric emission (Stappers et al. 2014). But, if for the LMXB state of J1023 the γ -ray emis-

sion is a part of this magnetospheric emission, then the observed $L_{\gamma, \text{LMXB}} > L_{\gamma, \text{RMSP}}$ indicates that the pulsar spin-down power ($L_{\text{SD, LMXB}}^{\text{PW}}$) in the LMXB state is greater than that ($L_{\text{SD, RMSP}}^{\text{PW}}$) in the RMSP state (see section 3.1). This can happen if there are more open magnetic field lines in the LMXB state than those in the RMSP state. But what can open more field lines in the LMXB state? As mentioned in section 2, according to simulations, when the accretion disc extends inside the pulsar magnetosphere, at least a fraction of the magnetic field lines intersecting the disc should be opened and remain opened (Parfrey et al. 2016; Parfrey & Tchekhovskoy 2017; Jaodand et al. 2016). This should enhance the pulsar spin-down torque and spin-down power at most by a factor of $(r_{\text{lc}}/r_m)^2$. Note that, for $L_{\text{SD, LMXB}}^{\text{PW}} > L_{\text{SD, RMSP}}^{\text{PW}}$, $\eta_{\text{LMXB}}/\eta_{\text{RMSP}} < 1$ (see section 3.1). Therefore, as $L_{\gamma, \text{LMXB}}/L_{\gamma, \text{RMSP}}$ can be as high as ~ 10 for J1023 (although Deller et al. (2015) reported a lower value (~ 6.5) of this ratio; section 1), $L_{\text{SD, LMXB}}^{\text{PW}}$ may be sometimes more than 10 times $L_{\text{SD, RMSP}}^{\text{PW}}$ for this source (using Eq. 7). Can our formalism explain these for J1023? As shown in section 4.2, our formalism leads to the conclusion that the accretion disc extends inside the pulsar magnetosphere in the LMXB state, and hence should enhance the spin-down power at most by a factor of $(r_{\text{lc}}/r_m)^2$, which is ≈ 10.7 (considering $r_m \sim r_{m, \text{high}} \approx 24.6 \text{ km}$) and ≈ 10 (considering $r_m \sim r_{\text{co}} \approx 25.4 \text{ km}$) using the example in section 4.2. Therefore, this formalism can explain the required increase of the pulsar spin-down power in the LMXB state. So it is feasible for the γ -ray emission to be a part of the pulsar magnetospheric emission in the LMXB state of J1023.

4.4 Main points of the formalism

We emphasize that our formalism and understanding of J1023 are based on three general equations (3, 4 and 7). Our main conclusion is, the gravitational wave emission from the pulsar is inevitable for $\eta_{\text{LMXB}}/\eta_{\text{RMSP}} < k$, where k is somewhat greater than 1 (see section 3.1). Therefore, as discussed before, if γ -rays are primarily a part of the pulsar magnetospheric emission in both RMSP and LMXB states (implying $\eta_{\text{LMXB}}/\eta_{\text{RMSP}} < 1$; section 3.1), our conclusion of gravitational wave emission from the pulsar in J1023 should be robust. While such a γ -ray production directly from the magnetospheric outflow and emission is natural and feasible in the RMSP state (see section 4.3), here we mention a few points to show that this production mechanism is quite likely even for the LMXB state.

- (1) If the active magnetosphere of a pulsar can directly produce γ -rays in the RMSP state, then if this magnetosphere remains active in the LMXB state, it might naturally keep on producing γ -rays in the latter state. Then this would be the simplest mechanism for the γ -ray production in the LMXB state, and an additional mechanism (e.g., by a pulsar wind – accretion disc collision; see section 2) would imply an additional model.
- (2) Currently, no observation significantly falsifies the magnetospheric production of γ -rays in the LMXB state. For example, no significant γ -ray spectral difference has been found between LMXB and RMSP states (Stappers et al. 2014).
- (3) In section 4.3, we have shown in detail that the magnetospheric γ -ray production mechanism in the LMXB state is feasible.

(4) While this production mechanism in our formalism can explain the energy budget, the torque budget and X-ray pulsations by the standard model, an alternative mechanism involving a pulsar wind – accretion disc collision may not explain all these (see section 2).

Furthermore, our formalism does not require an additional γ -ray production mechanism (e.g., by a pulsar wind – accretion disc collision), and it self-consistently explains some main observational aspects of J1023 for a γ -ray production directly from the pulsar magnetospheric outflow and emission. Here are two examples.

(1) Our formalism, based on Eqs. 3, 4 and 7 and a magnetospheric γ -ray production, infers accretion disc penetration into the pulsar magnetosphere in the LMXB state and accretion onto the neutron star in the high-mode. This, considering the opening of magnetic field lines, can naturally explain an increased magnetospheric γ -ray production in the LMXB state.

(2) The equatorial part of the pulsar wind may be switched off by the accretion disc penetrating the pulsar magnetosphere (see [Veledina et al. 2019](#)) in the LMXB state. Therefore, no significant collision between the pulsar wind and the accretion disc, and hence no γ -ray production from such a collision, are expected in our formalism. This is consistent with a magnetospheric γ -ray production.

4.5 Other observational aspects

While it is not our aim to probe all the observational aspects of J1023, several such aspects, as discussed above, can be comfortably explained using our formalism. However, there are some observational aspects, which have not been reliably understood so far by any model, and for these we can offer only speculative explanations. Here are some examples. The absence of observed radio pulsations in the LMXB state, when the pulsar magnetospheric activities are present, could be due to intra-binary material causing scattering and/or absorption ([Stappers et al. 2014](#)). The flat radio spectrum in the LMXB state indicated a jet ([Deller et al. 2015](#)), which, as shown by simulations, could be due to the pulsar wind collimated by the accretion flow ([Parfrey & Tchekhovskoy 2017](#)). Besides, the optical pulsations at the pulsar spin frequency ([Ambrosino et al. 2017](#)) could be explained in terms of the cyclotron emission from inflowing electrons in accretion columns within the accretion disc inner edge ([Papitto et al. 2019](#)). But, the accretion columns are expected to be optically thick, which would imply an optical luminosity more than an order of magnitude lower than the observed optical pulsed luminosity ($\sim 10^{31}$ erg s $^{-1}$; [Papitto et al. 2019](#)). We speculate that parts of the accretion columns are irradiated and puffed up by the energy from pulsar magnetospheric activities and become optically thin. This might explain the optical pulsed luminosity in terms of the cyclotron emission of electrons in accretion columns. Note that the corresponding energy budget can comfortably be explained, as the optical pulsed luminosity is orders of magnitude lower than the X-ray luminosity ($\sim 7 \times 10^{33}$ erg s $^{-1}$) due to accretion, as well as the γ -ray luminosity ($\sim (6 - 12) \times 10^{33}$ erg s $^{-1}$) powered by the pulsar spin-down through magnetospheric emission. This would also explain how the optical pulses originate within a few kilometers from the location of the X-ray pulse ori-

gin and why the optical pulses are observed only in high- and flaring-modes (see section 1), when accretion onto the pulsar happens according to our scenario. Moreover, optical pulsations have not been reported for other AMXPs yet, and hence this feature is likely uncommon for AMXPs, perhaps because pulsar magnetospheric activities are quenched for them in the accreting state (see section 4.3).

5 METHOD TO CONSTRAIN PARAMETER VALUES

In sections 3 and 4, we have presented our formalism and primary results in a simple manner for typical parameter values. In this section, we describe the method to constrain source parameter values, including neutron star magnetic dipole moment and misaligned mass quadrupole moment, following the formalism mentioned in section 3 and the discussion given in section 4. In order to make our results robust, we use full ranges of measured parameter values and entire expected ranges of other input parameter values, and include additional uncertainties for parameters such as accretion/ejection induced rate of change of spin frequency. To the best of our knowledge, hitherto a study of J1023 considering such large ranges of parameter values has not been done.

The input parameters are pulsar mass M , pulsar radius R , an order of unity constant ξ (Eq. 1), A (where, the pulsar moment of inertia $I = AMR^2$), the γ -ray luminosity $L_{\gamma, \text{LMXB}}$ in the LMXB state, the pulsar braking index n , the angle α between the magnetic and spin axes (Eq. 8), f_{Acc} (uncertainty factor of $\nu_{\text{LMXB}}^{\text{Acc}}$; Eq. 4), and $\eta_{\text{LMXB}}/\eta_{\text{RMSP}}$. The ranges of values explored for these parameters are $M : 1.55 - 1.87 M_{\odot}$ ([Deller et al. 2012](#)); $R : 8 - 16$ km (the largest plausible range; e.g., [Bhattacharyya et al. 2017](#)); $\xi : 0.3 - 1.0$ ([Patruno & Watts 2012](#)); $A : 0.33 - 0.43$ ([Bhattacharyya et al. 2017](#)); $L_{\gamma, \text{LMXB}} : (6.0 - 12.4) \times 10^{33}$ erg s $^{-1}$ ([Nolan et al. 2012](#); [Stappers et al. 2014](#); [Deller et al. 2015](#); [Torres et al. 2017](#)); $n : 1.4 - 3.0$ ([Lyne & Graham-Smith 2012](#)); $\alpha : 5^{\circ} - 90^{\circ}$ (\sim entire range); $f_{\text{Acc}} : 0.5 - 1.5$ (a large fractional uncertainty) and $\eta_{\text{LMXB}}/\eta_{\text{RMSP}} : \leq 3$ (a reasonably large range, including the range for primarily pulsar magnetospheric origin of γ -rays). In order to make our results reliable, we consider a large number ($\sim 1.8 \times 10^9$) of combinations of input parameter values within these ranges, and for each combination, estimate various source parameter values, including stellar magnetic dipole moment μ and misaligned mass quadrupole moment Q , following the formalism described in section 3 and the discussion given in section 4. In order to constrain the source parameter values, we impose the following conditions using observational aspects of J1023 (see section 4 for details). (1) $r_{\text{m,high}} \leq r_{\text{co}}$ and $r_{\text{m,low}} \geq r_{\text{co}}$, which are required to explain high- and low-modes, and the X-ray pulsations only in the high-mode using the standard mechanism. (2) In the RMSP state, the pulsar magnetospheric spin-down luminosity $L_{\text{SD, RMSP}}^{\text{PW}} \geq 3 \times 10^{33}$ erg s $^{-1}$, which is required to explain the observed irradiation of the companion star. (3) $(r_{\text{lc}}/r_{\text{co}})^2 > L_{\text{SD, LMXB}}^{\text{PW}}/L_{\text{SD, RMSP}}^{\text{PW}}$ (considering $r_{\text{m}} \sim r_{\text{co}}$), which is required for magnetic field lines opening to explain the increased pulsar magnetospheric production of γ -rays in the LMXB state. In addition, following the theoretical struc-

ture computations of MSPs (Bhattacharyya et al. 2017), we consider $10^{45} \text{ g cm}^2 \leq I \leq 4 \times 10^{45} \text{ g cm}^2$. The resulting constrained ranges of parameter values are reported in section 6.

6 CONSTRAINTS ON PARAMETER VALUES

Using our formalism (section 3) and discussion in section 4, full ranges of measured parameter values, and entire expected ranges of other input parameter values (see section 5), we constrain a number of parameters for J1023, and list their allowed values in Table 1. Such a systematic and extensive study of the parameter space of J1023 has not been done so far, to the best of our knowledge. Theoretical calculations predict that a neutron star could sustain a Q and an ϵ , which are orders of magnitude higher than $\sim 10^{36} \text{ g cm}^2$ and $\sim 10^{-9}$ respectively (Johnson-McDaniel & Owen 2013). Therefore, as the stellar gravity cannot iron out such an unevenness, structural imperfections should remain, and hence a net $\epsilon \sim 10^{-9}$ could naturally exist in neutron stars. For example, a buried strong magnetic field or a strain in the elastic crust could give rise to a non-zero ellipticity (Woan et al. 2018). Moreover, if such a natural ellipticity exists in the RMSP state of J1023, it should not disappear in the LMXB state. Therefore, without assuming an additional source of ellipticity in the latter state, we consider $\dot{\nu}_{\text{LMXB}}^{\text{GW}} = \dot{\nu}_{\text{RMSP}}^{\text{GW}}$ (implying $Q_{\text{LMXB}} = Q_{\text{RMSP}} = Q$ and $\epsilon_{\text{LMXB}} = \epsilon_{\text{RMSP}} = \epsilon$) for the first set of constraints in Table 1. We find $\mu \approx (2.5 - 4.4) \times 10^{25} \text{ G cm}^3$, implying $B \approx (0.7 - 6.1) \times 10^7 \text{ G}$, and $Q \approx (0.92 - 1.88) \times 10^{36} \text{ g cm}^2$, implying $\epsilon \approx (0.48 - 0.93) \times 10^{-9}$. The constrained $Q - \mu$ space is shown in Fig. 1.

While $Q_{\text{LMXB}} = Q_{\text{RMSP}}$ is the simplest possibility, let us now consider more general cases. If the pulsar ellipticity can increase in the LMXB state due to an additional accretion-related asymmetry, which requires an additional mechanism (see Haskell & Patruno (2017); Singh et al. (2020) for an example of a mechanism), then we get $Q_{\text{RMSP}} \approx (0.92 - 1.90) \times 10^{36} \text{ g cm}^2$ and $Q_{\text{LMXB}} \approx (0.92 - 2.20) \times 10^{36} \text{ g cm}^2$ (Table 1). Therefore, our formalism does not exclude a model of the pulsar ellipticity increase during accretion. However, depending on the relative orientations of the natural ellipticity and the accretion-related asymmetry, the net ellipticity could even decrease in the LMXB state. Therefore, without considering any mutual condition between $\dot{\nu}_{\text{RMSP}}^{\text{GW}}$ and $\dot{\nu}_{\text{LMXB}}^{\text{GW}}$, we find $Q_{\text{RMSP}} \approx (0.92 - 1.90) \times 10^{36} \text{ g cm}^2$ and $Q_{\text{LMXB}} \approx (0.39 - 2.20) \times 10^{36} \text{ g cm}^2$ (Table 1). These may imply that J1023 has a permanent ellipticity, and emits gravitational waves in both RMSP and LMXB states, even when we do not impose any constraints on $\dot{\nu}_{\text{RMSP}}^{\text{GW}}$ and $\dot{\nu}_{\text{LMXB}}^{\text{GW}}$.

What is the possibility of detection of gravitational waves from J1023? For MSPs ($\nu > 100 \text{ Hz}$) with ellipticities of 10^{-9} and the canonical moment of inertia (I), and for a one-year observation period with coherently combined data, Woan et al. (2018) have estimated the signal-to-noise ratios. We find that the ellipticity of the neutron star in J1023 could be somewhat less than 10^{-9} , but its ν -value is among the highest values observed for MSPs. Moreover, considering the numerically and general relativistically computed I -values for wide varieties of equation of state models for an MSP (PSR J1903+0327) of a comparable mass (see

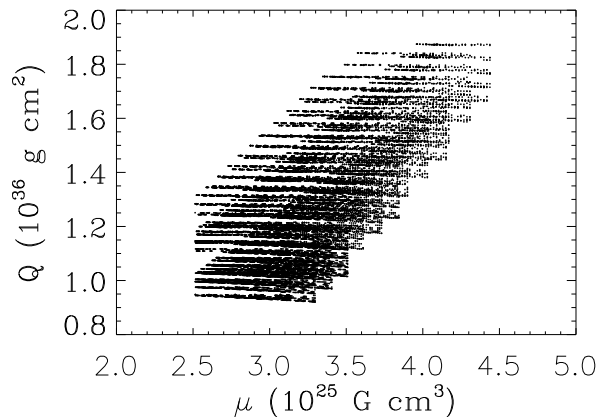


Figure 1. Constraint on the misaligned mass quadrupole moment (Q) versus magnetic dipole moment (μ) space for the pulsar PSR J1023+0038 (see section 6). Here, we use full ranges of measured parameter values, entire expected ranges of other input parameter values, and a few additional constraints (see section 5 for details). Besides, here we consider that Q is same in RMSP and LMXB states. The clustering of points is due to the chosen grid of parameters. The overall increase of Q with μ is due to the increase of the pulsar moment of inertia I , which is an input parameter (see Eqs. 8 and 9). For a given I -value, however, there is typically a weak anticorrelation between Q and μ , which is expected (see Eqs. 3, 8 and 9).

Table 3 of Bhattacharyya et al. 2017), we may assume that the I -value of J1023 could be around $(1.7 - 3) \times 10^{45} \text{ g cm}^2$, which is relatively high. Therefore, considering Fig. 2 of Woan et al. (2018), while it is unlikely that gravitational waves from J1023 would be detected with two upgraded advanced LIGO detectors, together with the advanced Virgo detector (Acernese et al. 2015), there could be a reasonable chance of detection with the Cosmic Explorer (Abbott et al. 2017) and the Einstein Telescope in its ET-D configuration (Hild et al. 2011; Sathyaprakash et al. 2012). Note that a plausible detection of continuous gravitational waves from J1023 and the corresponding estimation of Q in the future may confirm our formalism, infer some source parameter values using our method, and generally be useful to probe the physics of neutron stars, binary systems, accretion through a magnetosphere and stellar and binary evolutions.

7 SUMMARY

In this section, we summarize the main points of this paper. (1) A millisecond pulsar (MSP) could sustain a misaligned mass distribution or ellipticity around the spin-axis, and hence could emit continuous gravitational waves. An indirect way to infer such waves is to estimate the contribution of the waves to the spin-down rate of the pulsar. The transitional pulsar PSR J1023+0038 is so far the only MSP for which this spin-down rate has been measured in both the non-accreting radio MSP (RMSP) state and the accreting low-mass X-ray binary (LMXB) state. This unique information makes PSR J1023+0038 ideal to theoretically investigate if the pulsar has a non-zero ellipticity.

Table 1. Constraints on parameters of PSR J1023+0038 (see sections 5 and 6).

No.	Parameters ¹	For $\dot{\nu}_{\text{LMXB}}^{\text{GW}} = \dot{\nu}_{\text{RMSP}}^{\text{GW}}$ (with $\approx 0.2\%$ accuracy)	For $\dot{\nu}_{\text{LMXB}}^{\text{GW}} \geq \dot{\nu}_{\text{RMSP}}^{\text{GW}}$	No mutual condition between $\dot{\nu}_{\text{LMXB}}^{\text{GW}}, \dot{\nu}_{\text{RMSP}}^{\text{GW}}$
1	r_{co} (km)	24.6 – 26.2	24.6 – 26.2	24.6 – 26.2
2	$\text{Max}(R, r_{\text{ISCO}})$ (km)	14.0 – 16.8	14.0 – 16.8	14.0 – 16.8
3	$r_{\text{m,high}}$ (km)	20.2 – 26.2	19.4 – 26.2	19.4 – 26.2
4	$r_{\text{m,low}}$ (km)	24.6 – 32.5	24.6 – 32.5	24.6 – 32.5
5	$(r_{\text{lc}}/r_{\text{co}})^2$	9.5 – 10.7	9.5 – 10.7	9.5 – 10.7
6	$(r_{\text{lc}}/r_{\text{m,high}})^2$	9.5 – 15.9	9.5 – 17.2	9.5 – 17.2
7	μ (10^{25} G cm ³)	2.5 – 4.4	2.5 – 4.4	2.5 – 4.4
8	$\dot{\nu}_{\text{RMSP}}^{\text{PW}}$ (10^{-15} Hz s ⁻¹)	–0.067 to –0.217	–0.033 to –0.217	–0.033 to –0.217
9	$\dot{\nu}_{\text{LMXB}}^{\text{PW}}$ (10^{-15} Hz s ⁻¹)	–0.692 to –0.941	–0.066 to –0.941	–0.066 to –2.243
10	$\dot{\nu}_{\text{RMSP}}^{\text{GW}}$ (10^{-15} Hz s ⁻¹)	–1.673 to –1.823	–1.673 to –1.857	–1.673 to –1.857
11	$\dot{\nu}_{\text{LMXB}}^{\text{GW}}$ (10^{-15} Hz s ⁻¹)	–1.670 to –1.827	–1.673 to –2.484	–0.295 to –2.484
12	$\dot{\nu}_{\text{LMXB}}^{\text{Acc}}$ (10^{-15} Hz s ⁻¹)	0.015 to 0.114	0.014 to 0.114	0.014 to 0.114
13	$L_{\text{SD,RMSP}}^{\text{PW}}$ (10^{33} erg s ⁻¹)	3.00 – 9.36	3.00 – 9.36	3.00 – 9.36
14	η_{RMSP}	0.13 – 0.40	0.13 – 0.40	0.13 – 0.40
15	Q_{RMSP} (10^{36} g cm ²)	0.92 – 1.88	0.92 – 1.90	0.92 – 1.90
16	Q_{LMXB} (10^{36} g cm ²)	0.92 – 1.88	0.92 – 2.20	0.39 – 2.20

¹ $\text{Max}(R, r_{\text{ISCO}})$ is the larger of R and r_{ISCO} . Parameters are defined in the text.

(2) While we do not a priori assume a non-zero ellipticity of this pulsar, we can show that torque budget equations and pulsar magnetospheric origin of observed γ -rays in two states naturally infer such an ellipticity and continuous gravitational waves from PSR J1023+0038.

(3) Our formalism, which is basically independent of accretion, infers accretion disc penetration into the pulsar magnetosphere, and explains the observed X-ray pulsations in the LMXB state using the standard and well-accepted scenario. This, in turn, naturally infers the significantly larger pulsar spin-down power in the LMXB state, which we use in our formalism to explain the observed larger γ -ray emission in this state. This shows the self-consistency of our formalism.

(4) Finally, exploring large ranges of parameter values, and without assuming an additional source of ellipticity in the LMXB state, we infer a permanent misaligned mass quadrupole moment of the pulsar in the range $(0.92 - 1.88) \times 10^{36}$ g cm², implying the $(0.48 - 0.93) \times 10^{-9}$ range of ellipticity for PSR J1023+0038.

8 DATA AVAILABILITY

Observational data used in this paper are publicly available, and references are mentioned. The data generated from computations are already reported in this paper, and any additional used data will be available on request.

REFERENCES

- Abbott B. P., et al., 2017, CQGra, 34, 044001
 Abbott B. P., et al., 2019, ApJ, 879, 10
 Abdo A. A., et al., 2013, ApJS, 208, 17
 Acernese F., Agathos M., Agatsuma K., et al., 2015, CQGra, 32, 024001
 Ambrosino F., et al., 2017, Nature Astronomy, 1, 854
 Andersson N., Kokkotas K. D., Stergioulas N., 1999, ApJ, 516, 307
 Archibald A. M., et al., 2009, Science, 324, 1411
 Archibald A. M., Kaspi V. M., Bogdanov S., Hessels J. W. T., Stairs I. H., Ransom S. M., McLaughlin M. A., 2010, ApJ, 722, 88
 Archibald A. M., Kaspi V. M., Hessels J. W. T., Stappers B., Janssen G., Lyne A. G., 2013, Long-term radio timing observations of the transition millisecond pulsar PSR J1023+0038., arXiv:1311.5161

- Archibald A. M., et al., 2015, *ApJ*, 807, 62
- Bhattacharya D., van den Heuvel E. P. J., 1991, *Physics Reports*, 203, 1
- Bhattacharyya S., 2017, *ApJ*, 847, 2
- Bhattacharyya S., Chakrabarty D., 2017, *ApJ*, 835, 4
- Bhattacharyya S., Bombaci I., Bandyopadhyay D., Thampan A. V., Logoteta D., 2017, *New Astron.*, 54, 61
- Bildsten L., 1998, *ApJ*, 501, L89
- Bogdanov S., et al., 2015, *ApJ*, 806, 148
- Bozzo E., Ascenzi S., Ducci L., Papitto A., Burderi L., Stella L., 2018, *A&A*, 617, A126
- Campana S., Zelati F. C., Papitto A., Rea N., Torres D. F., Baglio M. C., D'Avanzo P., 2016, *A&A*, 594, A31
- Chakrabarty D., et al., 2003, *Nature*, 424, 42
- D'Angelo C. R., Spruit H. C., 2010, *MNRAS*, 406, 1208
- Deller A. T., et al., 2012, *ApJ*, 756, L25
- Deller A. T., et al., 2015, *ApJ*, 809, 13
- Haskell B., Patruno A., 2017, *Phys. Rev. Lett.*, 119, 161103
- Hild S., Abernathy M., Acernese F., et al., 2011, *CQGra*, 28, 094013
- Jaodand A., Archibald A. M., Hessels J. W. T., Bogdanov S., D'Angelo C. R., Patruno A., Bassa C., Deller A. T., 2016, *ApJ*, 830, 122
- Johnson-McDaniel N. K., Owen B. J., 2013, *Phys. Rev. D*, 88, 044004
- Kennedy M. R., Clark C. J., Voisin G., Breton R. P., 2018, *MNRAS*, 477, 1120
- Lyne A., Graham-Smith F., 2012, *Pulsar Astronomy*. Cambridge University Press
- Nolan P. L., et al., 2012, *ApJS*, 199, 31
- Papitto A., Torres D. F., 2015, *ApJ*, 807, 33
- Papitto A., et al., 2019, *ApJ*, 882, 104
- Parfrey K., Tchekhovskoy A., 2017, *ApJ*, 851, L34
- Parfrey K., Spitkovsky A., Beloborodov A. M., 2016, *ApJ*, 822, 33
- Patruno A., Watts A. L., 2012, in Belloni T., Mendez M., Zhang C. M., eds., *Timing neutron stars: pulsations, oscillations and explosions*. ASSL, Springer
- Sathyaprakash B., Abernathy M., Acernese F., et al., 2012, *CQGra*, 29, 124013
- Singh N., Haskell B., Mukherjee D., Bulik T., 2020, *MNRAS*, 493, 3866
- Stappers B. W., et al., 2014, *ApJ*, 790, 39
- Takata J., et al., 2014, *ApJ*, 785, 131
- Tendulkar S. P., et al., 2014, *ApJ*, 791, 77
- Thorstensen J. R., Armstrong E., 2005, *Astron. J.*, 130, 759
- Torres D. F., Ji L., Li J., Papitto A., Rea N., de Oña Wilhelmi E., Zhang S., 2017, *ApJ*, 836, 68
- Veledina A., Nattila J., Beloborodov A. M., 2019, *ApJ*, 884, 144
- Wang Y.-M., 1996, *ApJ*, 465, L111
- Wang Z., Archibald A. M., Thorstensen J. R., Kaspi V. M., Lorimer D. R., Stairs I., Ransom S. M., 2009, *ApJ*, 703, 2017
- Woon G., Pitkin M. D., Haskell B., Jones D. I., Lasky P. D., 2018, *ApJ*, 863, L40
- Zelati F. C., et al., 2014, *MNRAS*, 444, 1783
- Zelati F. C., Campana S., Braitto V., Baglio M. C., D'Avanzo P., Rea N., Torres D. F., 2018, *A&A*, 611, A14

This paper has been typeset from a $\text{\TeX}/\text{\LaTeX}$ file prepared by the author.